Supporting Information

X-ray-Triggered Through-space Charge Transfer and Photochromism in Silver Nanoclusters

Zhen Ren[a§], Jun-Jun Sun[a§], Long Xu[c], Peng Luo[a], Zi-Wei Ma[a], Si Li[b], Yu-Bing Si[b], Xi-Yan Dong[a,b,*], Fangfang Pan[c,*]

[a] *College of Chemistry and Chemical Engineering, Henan Polytechnic University, Jiaozuo 454000,China*

[b] *College of Chemistry, Zhengzhou University, Zhengzhou 450001, China*

[c] *College of Chemistry, Central China Normal University, Wuhan 430079, China*

Materials and chemicals.

All chemicals and solvents obtained from suppliers were used without further purification. Ethanol (EtOH, 99.5%), Methanol (99.5%), Silver oxide (Ag_2O, 99.7%), 3,3-Dimethyl-1-butyne ($^tBuC{\equiv}CH$, 95%), Ammonium hydroxide solution (NH_4OH, 28%), Silver trifluoroacetate ($AgC_2F_3O_2$, 98%), Silver tetrafluoroborate ($AgBF_4$, 99%), Acetonitrile (CH_3CN, 99.5%), Sodium chloride (NaCl, 99.5%), N,N-Dimethylformamide (DMF, 99.5%) were obtained from Macklin.

Crystallographic data collection and structural refinement.

Single-crystal X-ray diffraction measurement of **Ag_{14}-II** were performed on a Rigaku XtaLAB Pro diffractometer with Cu-*Kα* radiation (*λ* = 1.54184 Å), Mo-*K*α radiation (λ = 0.71073 Å) at 200 K and Bruker APEX-II CCD diffractometer with Ga-*Kα* radiation (*λ* = 1.34139 Å) at 100 K and 300K. Cl@Ag14BF4 were performed on a Rigaku XtaLAB Pro diffractometer with Mo-*K*α radiation (λ = 0.71073 Å) at 200 K. F@Ag14OH and Br@Ag14OH were performed on a Bruker APEX-II CCD diffractometer with Ga-*Kα* radiation (*λ* = 1.34139 Å) at 100 K. **Ag_{14}-I** were performed on a Bruker APEX-II CCD diffractometer with Ga-*Kα* radiation (*λ* = 1.34139 Å) at 100 K. Data collection and reduction were performed using the program CrysAlisPro [1]. The structures were solved with direct methods (*SHELXS*) [2] and refined by full-matrix least squares on F^2 using *OLEX2* [3], which utilizes the SHELXL-2015 module [4]. All non-hydrogen atoms were refined anisotropically, and the hydrogen atoms were placed in idealized position. The crystal structures are visualized by DIAMOND 3.2 [5]. Detailed information on the crystal data, data collection and refinement data for Ag_{14} are summarized in Table S1, S2, S3, S4 and S6.

DFT calculation.

To provide a better understanding of the photophysical properties of Ag cluster, the excited states were simulated by density functional theory (DFT) / time-dependent density functional theory (TDDFT) at PBE0/def2-SVP theoretical level with use of Q-Chem program [6]. Firstly, the ground state of Ag cluster was optimized based on the crystal structure, then the UV-Vis spectrum was mimicked at the same theoretical level. Considering the inner-sphere electron transfer was involved in the mixed-valent complex, the constrained density functional theory (CDFT) was thus employed to construct the excited state which triggered by X-ray spectrum [7]. Although the

Ag(0) was possibly contained in the compound, in the CDFT calculation, the charge of Ag still be set as 0.6 for the sake of convergence. The electrostatic potential surface and the molecular orbitals were calculated and visualized by Multiwfn program [8].

Experimental Section.

Synthesis of $(^t$BuAgC≡C$)_n$: Ag_2O (1 g, 4.3 mmol) was weighed into a 100 mL flask, and 50 mL of ammonium hydroxide was added. The solution was filtered after stirring for 10 min when almost all the silver oxide was dissolved. Then 3,3-dimethyL-1-butyne (1164 μL, 9.46 mmol) in 5 mL of ethanol was added to the solution under stirring, and white precipitate was formed immediately. After stirring in the dark for 30min, the whilte preciapitate with solution was filtered and subsquently washed with water, ethanol and ether to give 1.2 g $(^t$BuAgC≡C$)_n$ (74% yield based on Ag).

Caution! Due to the explosive nature of silver alkynyls, great care should be taken and only small amounts should be used.

Synthesis of Cl@Ag14BF_4: $AgBF_4$ (20 mg, 0.1 mmol) and $(^t$BuAgC≡C$)_n$ (78 mg, 0.4 mmol) was dissolved in 5 mL CH_3OHunder ultrasonication. To the resulting solution NaCl (3 mg, 0.05 mmol) was added. The mixture was sealed and heated 70 ºC for 24h. After cooled to room temperature, the colorless solution was filtered and the filtrate was evaporated slowly in air at room temperature in the dark. Approximately three days later, colorless prismatic block crystals appeared at the bottom of the bottle. Yield: 60% (63.0 mg) (based on $(^t$BuAgC≡C$)_n$). Elemental analysis (found (calculated), %; based on $C_{72}H_{108}ClBF_4Ag_{14}$: C, 33.23 (33.18); H, 4.20 (4.18).

The compounds, $[F@Ag_{14}(C{\equiv}C^tBu)_{12}]OH$, and $[Br@Ag_{14}(C{\equiv}C^tBu)_{12}]OH$ were synthesized based on previous reports [9][10].

All of the Ag_{14}-M-X in the picture represent Ag_{14}-M after Cu-$K\alpha_1$ X-ray irradiation!

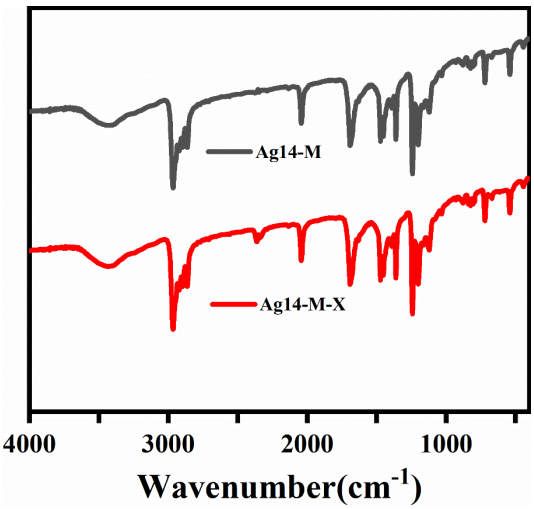

Fig. S1. Fourier-transform infrared spectroscopy (FTIR) of **Ag_{14}-M** before and after Cu-$K\alpha_1$ X-ray irradiation.
The anomalous peak appearing at the 2300 position is attributed to instrumental error .

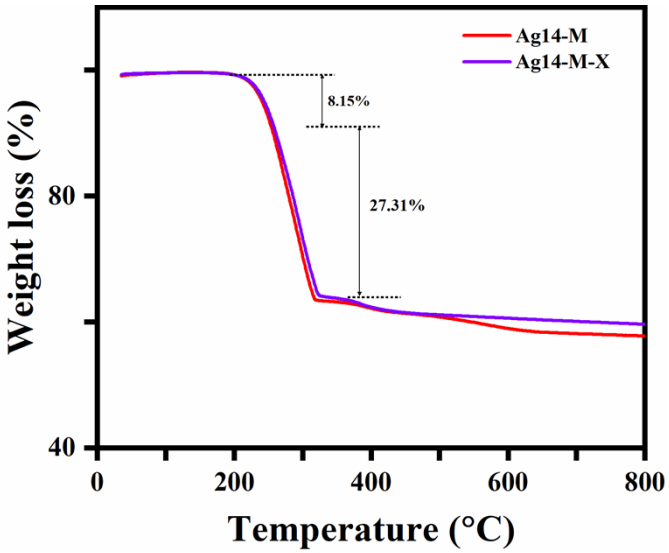

Fig. S2. TG curves of **Ag_{14}-M** and **Ag_{14}-M-X** under N_2 atmosphere with a heating rate of 10 °C/min.

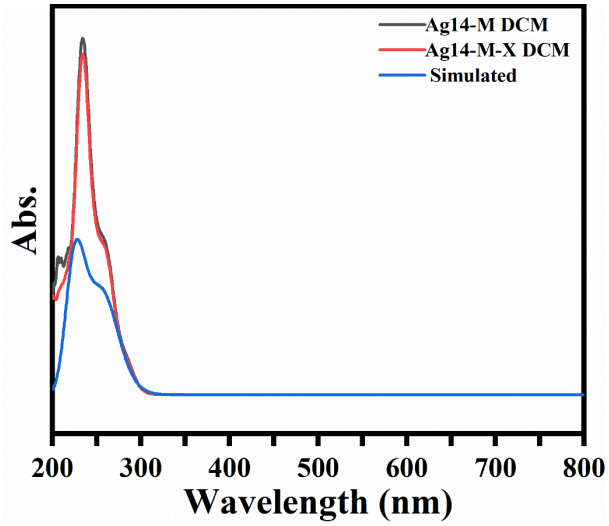

Fig. S3. Experimental and calculated absorption spectra of **Ag_{14}-M** cluster in CH_2Cl_2 at room temperature.

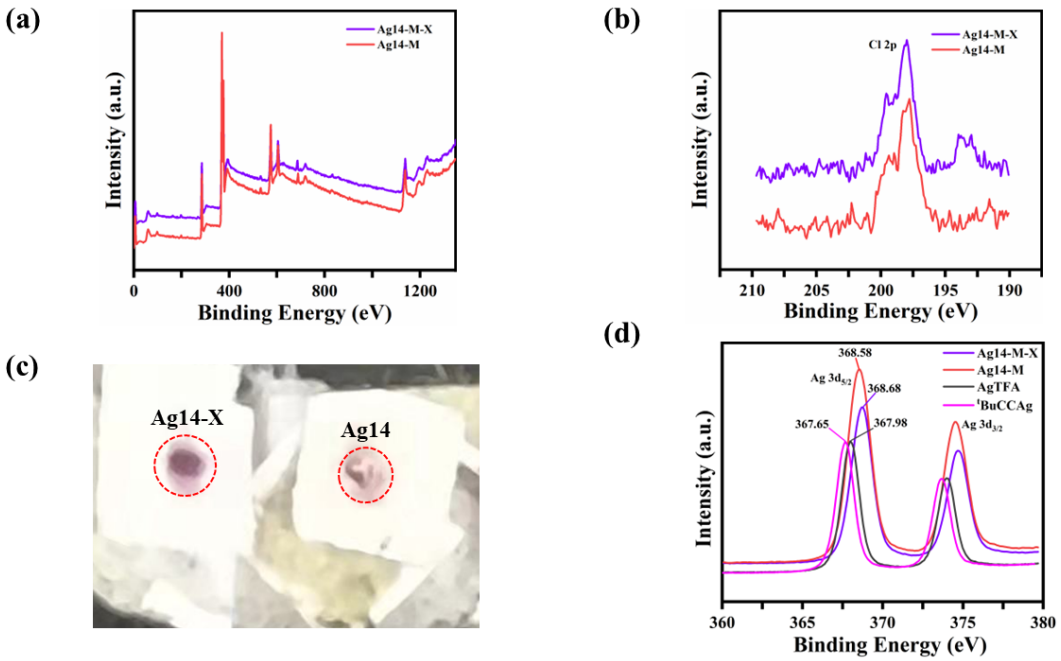

Fig. S4. (a) Survey XPS spectrum of **Ag_{14}-M** before and after Cu-$K\alpha_1$ X-ray irradiation. (b) XPS of Cl 2p. (c) The powder of **Ag_{14}-M** after Al-$K\alpha$ irradiation. (d) XPS signals of Ag3d for original **Ag_{14}-M** (red line), **Ag_{14}-M** after X-ray striking (**Ag_{14}-M-X**) (purple line), AgTFA (Black line) and ^{t}BuC≡CAg (Magenta line).

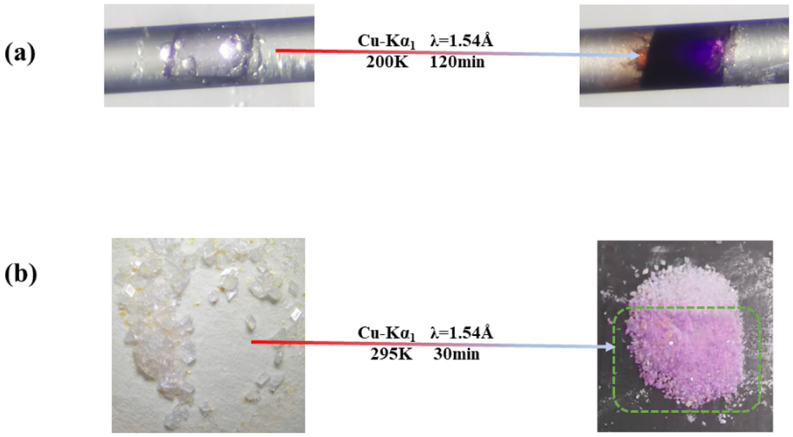

Fig. S5. (a) **Ag_{14}-II** crystal was induced photochromism by X-rays in mother liquor. (b) **Ag_{14}-M** crystal was induced photochromism by X-rays in the atmosphere.

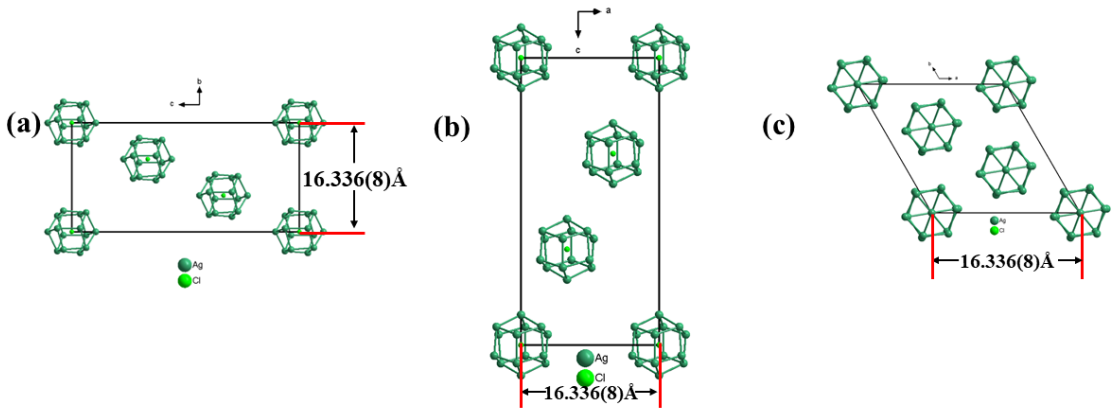

Fig. S6. The stacking pattern of the **Ag_{14}-II** along the a (a), b (b) and c (c) axis. The most recent inter-cluster distance is 16.336(8) Å

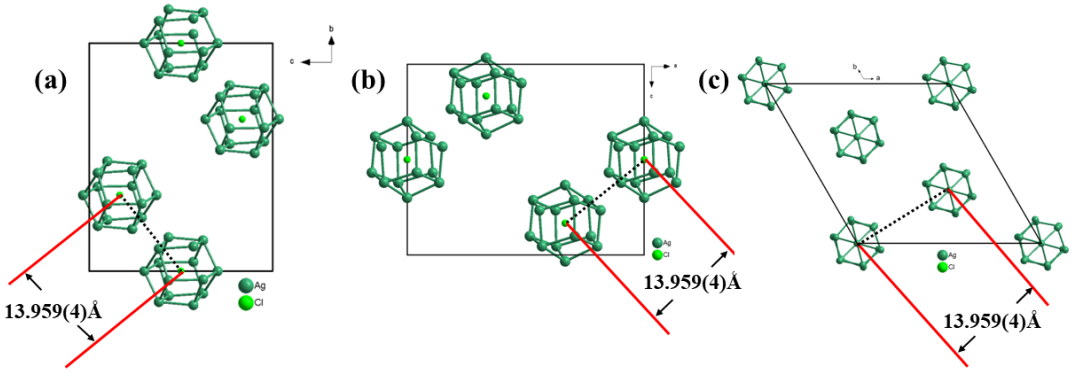

Fig. S7. The stacking pattern of the **Ag_{14}-I** along the a (a), b (b) and c (c) axis. The most recent inter-cluster distance is 13.959(4) Å

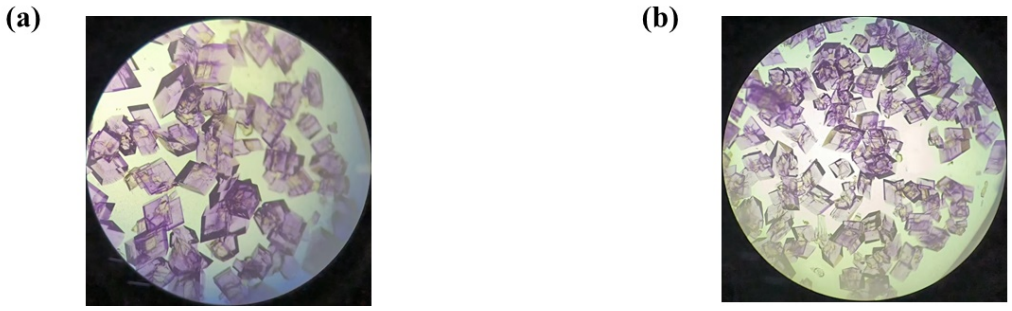

Fig. S8. (a) **Ag_{14}-M-X** heating at 60℃ under visible light for 24h. (b) **Ag_{14}-M-X** keeping in darkness for 24h.

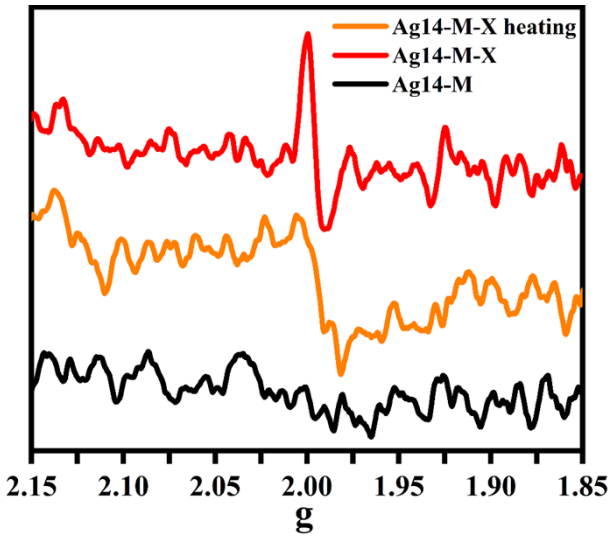

Fig. S9. Electron spin resonance (ESR) spectrum of **Ag_{14}-M**, **Ag_{14}-M-X** and **Ag_{14}-M-X** after heating. Due to the sample was slightly damaged after heating, the signal was not consistent with that before heating, but the signal did not disappear.

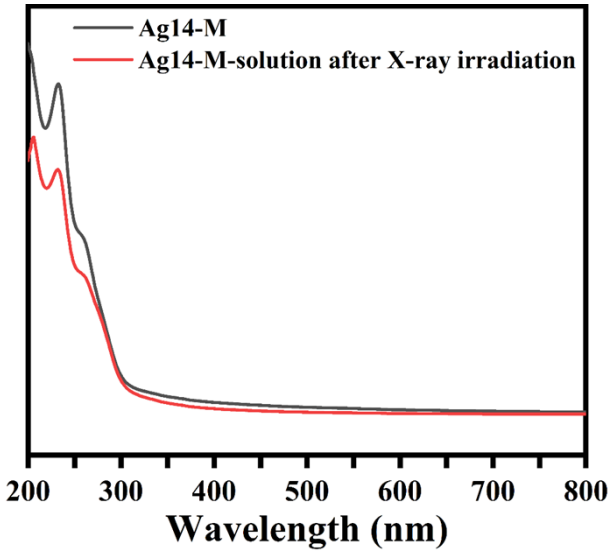

Fig. S10. UV–vis absorption spectrum of **Ag_{14}-M** in MeOH before and after X-ray irradiation.

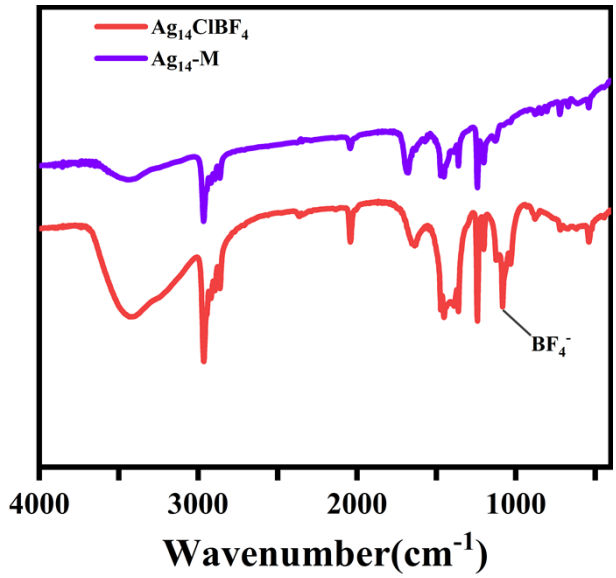

Fig. S11. FTIR of **Ag_{14}-M** and $Ag_{14}ClBF_4$, the peak in 1083cm^{-1} is BF_4^-.

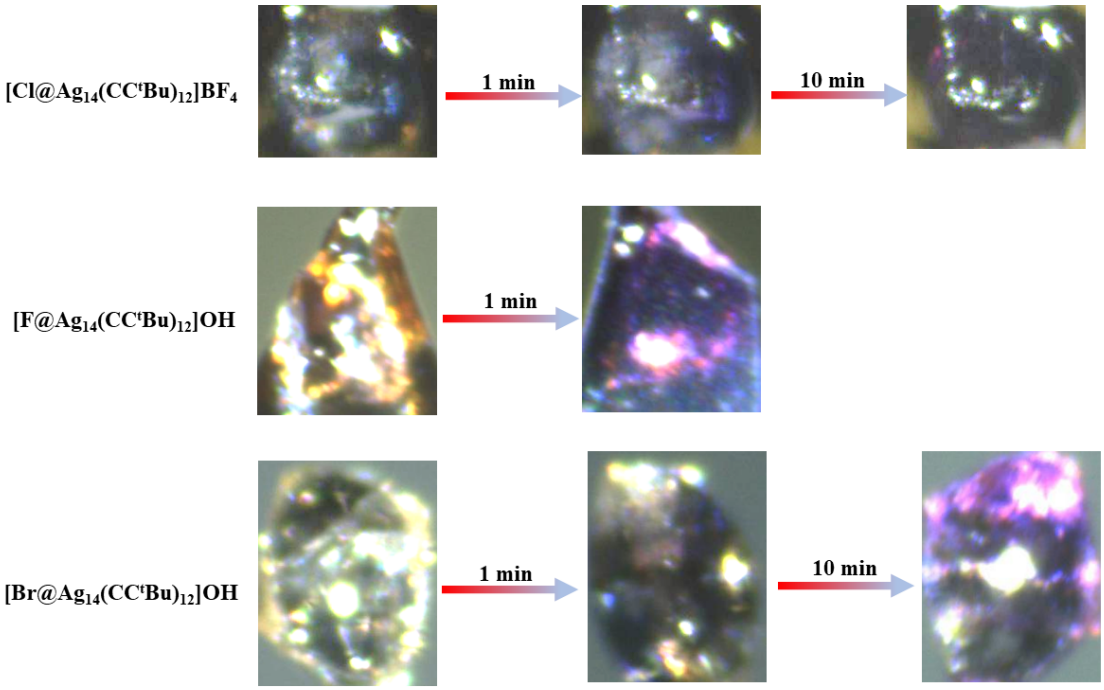

Fig. S12. Cl@$Ag_{14}BF_4$, F@$Ag_{14}OH$, Br@$Ag_{14}OH$ was induced photochromism respectively after being irradiated by Ga-$K\alpha_1$.

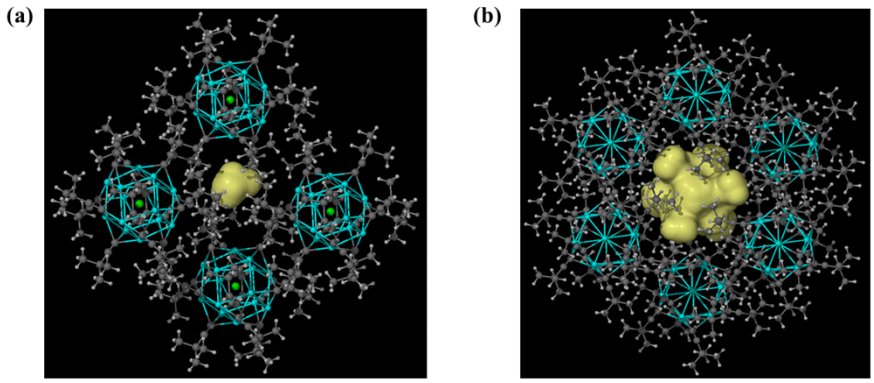

Fig. S13. The independent lattice void in **Ag_{14}-I** (a) **and Ag_{14}-II** (b), the yellow areas are voids.

Table S1. Crystal data and structure refinement of **Ag_{14}-I** which reported and collected with Ga-*K*α.

Compound	**Ag_{14}-I**[a]	**Ag_{14}-I-Ga**[b]
CCDC	163113	2284351
Empirical formula	C72H109OClAg14	C72H109Ag14ClO
Formula weight	2536.22	2536.22
Temperature/K	293(2)	100
Crystal system	Rhombohedral	trigonal
Space group	*R-3*	*R-3*
a/Å	22.438(2)	21.8873(7)
b/Å	22.438(2)	21.8873(7)
c/Å	15.601(2)	15.5998(8)
α/°	90	90
β/°	90	90
γ/°	120	120
Volume/Å^3	6801.8(13)	6471.9(5)
Z	3	3
ρ_{calc}g/cm^3	1.858	1.952
μ/mm^{-1}	3.010	17.327
F(000)	3672	3672
Radiation	Mo K*α* (λ = 0.71073)	Ga K*α* (λ = 1.34139)
2*θ* range for data collection/°	3.64 to 50	9.5 to 123.482
Index ranges	$0 \le h \le 25$, $-26 \le k \le 0$, $0 \le l \le 18$	$-28 \le h \le 26$, $-25 \le k \le 27$, $-20 \le l \le 20$
Reflections collected	2823	16626
Independent reflections	2618 [R_{int} = 0.0353, R_{sigma} = 0.0660]	3352 [R_{int} = 0.0674, R_{sigma} = 0.0517]
Data/restraints/parameters	2618/234/156	3352/126/197
Goodness-of-fit on F^2	------	1.192
Final *R* indexes [I>=2σ (I)]	R_1[c] = ------, wR_2 =-----	R_1 = 0.0969, wR_2 = 0.2236
Final *R* indexes [all data]	R_1 = 0.1332, wR_2 = -----	R_1 = 0.1041, wR_2 = 0.2266
Largest diff. peak/hole / e Å^{-3}	0.78/-0.44	1.73/-2.12

[a]The reported **Ag_{14}-I**.

[b]The parameters of **Ag_{14}-I** collected with Ga-*K*α.

[c]$R_1 = \sum||F_o| - |F_c||/\sum|F_o|$. $wR_2 = \{\sum[w(F_o^2 - F_c^2)^2]/\sum[w(F_o^2)^2]\}^{1/2}$.

Table S2. Typical bond length [Å] and angle [°] of **Ag_{14}-Mo**, **Ag_{14}-Cu-1** and **Ag_{14}-Cu-2**.

Bond distance/angle	Ag_{14}-II-Mo	Bond distance/angle	Ag_{14}-II-Cu-1	Bond distance/angle	Ag_{14}-II-Cu-2
Ag1-Ag2	2.9443(5)	**Ag1-Ag2**	2.9412(6)	**Ag1-Ag2**	2.9414(10)
Ag1-Ag3	2.920(4)	**Ag1-Ag3**	2.938(3)	**Ag1-Ag3^{i}**	2.942(3)
Ag1-Ag3^{b}	2.842(4)	**Ag1-Ag3^{e}**	2.937(3)	**Ag1-Ag3**	2.942(3)
Ag1-Ag3^{a}	2.959(3)	**Ag1-Ag3^{f}**	2.876(3)	**Ag1-Ag3^{j}**	2.886(5)
Ag2 -Ag1- Ag3^{a}	118.11(10)	**Ag2 -Ag1- Ag3**	73.97(6)	**Ag2 -Ag1- Ag3**	74.05(9)
Ag2 -Ag1 -Ag3^{b}	74.31(9)	**Ag2 -Ag1 -Ag3^{f}**	118.52(11)	**Ag2 -Ag1 -Ag3^{i}**	118.58(15)
Ag3 -Ag1 -Ag2	73.18(9)	**Ag3^{e} -Ag1 -Ag2**	74.88(6)	**Ag3^{j} -Ag1 -Ag2**	74.88(7)
Ag3^{b} -Ag1 -Ag3	118.37(15)	**Ag3^{e} -Ag1 -Ag3**	118.52(2)	**Ag3^{j} -Ag1 -Ag3^{i}**	118.8(3)
Ag3 -Ag1 -Ag3^{a}	75.14(7)	**Ag3^{f} -Ag1 -Ag3**	74.80(10)	**Ag3 -Ag1 -Ag3^{i}**	75.01(13)
Ag3^{a} -Ag1 -Ag3^{b}	76.31(7)	**Ag3^{f} -Ag1 -Ag3^{e}**	75.74(10)	**Ag3^{j}-Ag1 -Ag3**	75.85(11)
Ag1^{b} -Ag2 -Ag1	103.867(18)	**Ag^{j} -Ag2 -Ag1**	104.04(2)	**Ag1^{k} -Ag2 -Ag1**	104.18(4)
Ag1^{c} -Ag2 -Ag1	103.868(18)	**Ag^{j} -Ag2 -Ag1^{f}**	104.04(2)	**Ag1^{k} -Ag2 -Ag1^{j}**	104.18(4)
Ag1^{c} -Ag2 -Ag1^{b}	103.870(18)	**Ag1^{f} -Ag2 -Ag1**	104.04(2)	**Ag1^{j} -Ag2 -Ag1**	104.18(4)
Ag1 -Ag3 -Ag1^{d}	102.96(9)	**Ag1^{h} -Ag3 -Ag1**	103.50(12)	**Ag1^{k} -Ag3 -Ag1^{l}**	104.78(17)
Ag1^{c} -Ag3 -Ag1	107.13(17)	**Ag1^{h} -Ag3 -Ag1^{g}**	105.06(13)	**Ag1 -Ag3 -Ag1^{l}**	103.38(13)
Ag1^{c} -Ag3 -Ag1^{d}	104.90(9)	**Ag1^{g} -Ag3 -Ag1**	105.77(13)	**Ag1^{k} -Ag3 -Ag1**	105.55(19)

Symmetry codes: a: 1/3-Y+X,-1/3+X,2/3-Z b: 1-Y,+X-Y,+Z c: 1+Y-X,1-X,+Z d: 1/3+Y,2/3-X+Y,2/3-Z
e: -1/3+Y,1/3-X+Y,4/3-Z f: +Y-X,1-X,+Z g: 1-Y,1+X-Y,+Z h: 2/3-Y+X,1/3+X,4/3-Z
i: -1/3+Y,1/3-X+Y,4/3-Z j: +Y-X,1-X,+Z k: 1-Y,1+X-Y,+Z l: 2/3-Y+X,1/3+X,4/3-Z

Table S3. Crystal data and structure refinement of Ag_{14} collected with Ga-*K*α under different temperature.

Compound	Ag_{14}-II-Ga-100K	Ag_{14}- II-Ga-302K
CCDC	2303298	2303299
Empirical formula	C72H109OClAg14	C72H109Ag14ClO
Formula weight	2536.22	2536.22
Temperature/K	100	302
Crystal system	trigonal	trigonal
Space group	*R-3*	*R-3*
a/Å	16.1523(6)	16.438(3)
b/Å	16.1523(6)	16.438(3)
c/Å	29.3979(16)	29.900(7)
α/°	90	90
β/°	90	90
γ/°	120	120
Volume/Å^3	6642.3(6)	6996(3)
Z	3	3
ρ_{calc}g/cm^3	1.936	1.806
μ/mm^{-1}	16.891	16.028
F(000)	3753.0	3672
Radiation	Ga K*α* (λ = 1.34139)	Ga K*α* (λ = 1.34139)
2*θ* range for data collection/°	9.528 to 106.126	9.362 to 84.986
Index ranges	-18 ≤ h ≤ 19, -19 ≤ k ≤ 15, -20 ≤ l ≤ 34	-16 ≤ h ≤ 15, -16 ≤ k ≤ 16, -27 ≤ l ≤ 30
Reflections collected	12933	7045
Independent reflections	2598 [R_{int} = 0.0630, R_{sigma} = 0.0438]	1645 [R_{int} = 0.0660, R_{sigma} = 0.0493]
Data/restraints/parameters	2598/174/208	1645/102/169
Goodness-of-fit on F^2	1.057	1.072
Final *R* indexes [*I*>=2*σ* (*I*)]	R_1[a] = 0.0653, wR_2 = 0.1843	R_1 = 0.0660, wR_2 = 0.1889
Final *R* indexes [all data]	R_1 = 0.0758, wR_2 = 0.1940	R_1 = 0.0769, wR_2 = 0.2001
Largest diff. peak/hole / e Å^{-3}	1.19/-1.35	1.03/-1.02

[a]$R_1 = \sum||F_o| - |F_c||/\sum|F_o|$. $wR_2 = \{\sum[w(F_o^2 - F_c^2)^2]/\sum[w(F_o^2)^2]\}^{1/2}$.

Table S4. Typical bond length [Å] and angle [°] of **Ag_{14}-II-Ga-100K** and **Ag_{14}-II-Ga-302K**

Bond distance/angle	Ag_{14}-II-Ga-100K	Bond distance/angle	Ag_{14}-II-Ga-302K
Ag1-Ag2	2.9324(9)	**Ag1-Ag3**	2.9494(15)
Ag1-Ag3	2.873(3)	**Ag1-Ag2**	2.9631(16)
Ag1-Ag3^{a}	2.924(3)	**Ag1-Ag2^{e}**	2.9102(16)
Ag1-Ag3^{b}	2.9382(19)	**Ag1-Ag2^{f}**	2.982(2)
Ag3 -Ag1- Ag3^{a}	75.82(8)	**Ag2^{f} -Ag1- Ag2^{e}**	76.45(4)
Ag3^{a} -Ag1 -Ag3^{b}	74.83(10)	**Ag2 -Ag1 -Ag2^{f}**	75.66(4)
Ag3 -Ag1 -Ag3^{b}	118.68(19)	**Ag2^{e} -Ag1 -Ag2**	120.30(6)
Ag3 -Ag1 -Ag2	74.96(4)	**Ag2^{e} -Ag1 -Ag3**	75.29(4)
Ag2 -Ag1 -Ag3^{a}	118.55(10)	**Ag2^{f} -Ag1 -Ag3**	119.47(6)
Ag2 -Ag1 -Ag3^{b}	73.99(6)	**Ag3 -Ag1 -Ag2**	74.51(4)
Ag1^{b} -Ag2 -Ag1	104.18(3)	**Ag1^{g} -Ag2 -Ag1**	104.62(6)
Ag1^{d} -Ag2 -Ag1	104.18(3)	**Ag1^{g} -Ag2 -Ag1^{f}**	103.91(5)
Ag1^{d} -Ag2-Ag1^{b}	104.18(3)	**Ag1^{h} -Ag2 -Ag1**	102.63(5)
Ag1 -Ag3 -Ag1^{d}	105.55(12)	**Ag1^{e} -Ag3 -Ag1**	103.99(5)
Ag1^{c} -Ag3 -Ag1	105.02(13)	**Ag1^{g} -Ag3 -Ag1**	103.99(5)
Ag1^{c} -Ag3 -Ag1^{d}	103.37(10)	**Ag1^{g} -Ag3-Ag1$^{\backslash}$**	103.99(5)

Symmetry codes: a: -1/3+Y,1/3-X+Y,4/3-Z b: +Y-X,1-X,+Z c: 2/3-Y+X,1/3+X,4/3-Z d: 1-Y,1+X-Y,+Z e: 1/3-Y+X,-1/3+X,2/3-Z f: 1-Y,+X-Y,+Z g: 1+Y-X,1-X,+Z h: 1/3+Y,2/3-X+Y,2/3-Z

Table S5. XPS Ag $3d_{5/2}$ peak binding energy range for Ag(0) and Ag(I) states.

S. No.	compound	Ag $3d_{5/2}$ position (in eV) for Ag^0	Ag $3d_{5/2}$ position (in eV) for Ag^I	Reference
1	Ag, Ag_2CO_3	367.9	367.3	Anal. Chem. 1975, 47, 2193
2	Ag, Ag_2O	368.0	367.7	J. Phys. Chem. 1994, 98, 8519
3	Ag, Ag_2O	368.4	367.9	Nano Lett. 2005, 5, 2319
4	Ag, AgBr	368.3	367.5	ACS Nano 2011, 5, 4529
5	Ag, Ag_2S	368.2	367.8	Angew. Chem. Int. Ed. 2012, 51, 11501
6	$(PDDA/PSS)_5$/2Au@2Ag	368.4	---	Adv. Mater. 2012, 24, 4574
7	$[Ag_{15}Cu_6(C{\equiv}CR)_{18}(DPPE)_2]^-$	368.1	---	J. Am. Chem. Soc. 2023, 145, 6, 3401–3407
8	$[Ag_{22}Cu_7(C{\equiv}CR)_{16}(PPh_3)_5Cl_6](PPh_4)$	368.0	---	Angew. Chem. 2023, 135, e202217483
9	$Ag_{12}Cu_4(C{\equiv}CR)_{14}(PPh_3)_4$	368.1	----	J. Phys. Chem. C 2022, 126, 20577−20583
10	$[PdHAg_{19}(S_2P(O^iPr)_2)_{12}]$	368.43	----	Chem. Eur. J. 2023, 29, e202300730

Table S6. Crystal data and structure refinement of Ag_{14}-F-OH, Ag_{14}-Br-OH and Ag_{14}-Cl-BF_4 collected with Ga-*K*α

Compound	Ag_{14}-F-OH	Ag_{14}-Br-OH	Ag_{14}-Cl-BF_4
CCDC	2313779	2313778	2314495
Empirical formula	C72H109OFAg14	C72H109Ag14BrO	C72H109Ag14ClBF4
Formula weight	2519.77	2580.68	2606.02
Temperature/K	100	100	200.01(10)
Crystal system	trigonal	trigonal	trigonal
Space group	*R-3*	*R-3*	*R-3*
a/Å	21.8992(8)	21.9600(6)	16.5410(9)
b/Å	21.8992(8)	21.9600(6)	16.5410(9)
c/Å	15.4850(8)	15.4656(7)	29.8249(19)
α/°	90	90	90
β/°	90	90	90
γ/°	120	120	120
Volume/Å^3	6431.3(6)	6458.9(5)	7067.0(9)
Z	3	3	3
ρ_{calc}g/cm^3	1.952	1.990	1.837
μ/mm^{-1}	16.949	17.533	2.905
F(000)	3648.0	3726.0	3768.0
Radiation	Ga Kα (λ = 1.34139)	Ga Kα (λ = 1.34139)	Mo Kα (λ = 0.71073)
2θ range for data collection/°	9.514 to 110.99	9.498 to 116.042	3.942 to 57.514
Index ranges	-26 ≤ h ≤ 25, -23 ≤ k ≤ 26, -19 ≤ l ≤ 16	-23 ≤ h ≤ 25, -27 ≤ k ≤ 27, -19 ≤ l ≤ 18	-21 ≤ h ≤ 21, -21 ≤ k ≤ 18, -40 ≤ l ≤ 29
Reflections collected	18282	16450	9459
Independent reflections	2778 [R_{int} = 0.0609, R_{sigma} = 0.0431]	2878 [R_{int} = 0.0559, R_{sigma} = 0.0448]	3550 [R_{int} = 0.0378, R_{sigma} = 0.0378]
Data/restraints/parameters	2778/57/169	2878/87/166	3550/162/194
Goodness-of-fit on F^2	1.070	1.075	1.060
Final *R* indexes [I>=2σ (I)]	R_1[a] = 0.0501, wR_2 = 0.1320	R_1 = 0.0496, wR_2 = 0.1435	R_1 = 0.0466, wR_2 = 0.1364
Final *R* indexes [all data]	R_1 = 0.0745, wR_2 = 0.1446	R_1 = 0.0674, wR_2 = 0.1528	R_1 = 0.0698, wR_2 = 0.1480
Largest diff. peak/hole / e Å^{-3}	1.58/-1.39	1.00/-0.99	0.64/-0.60

[a]$R_1 = \sum||F_o| - |F_c||/\sum|F_o|$. $wR_2 = \{\sum[w(F_o^2 - F_c^2)^2]/\sum[w(F_o^2)^2]\}^{1/2}$.

Supplementary References

[1] CrysAlis^{Pro} Version 1.171.36.31. Agilent Technologies Inc. Santa Clara, CA, USA, 2012.

[2] G. M. Sheldrick, Acta Cryst. A 64 (2008) 112-122.

[3] O. V. Dolomanov, L. J. Bourhis, R. J. Gildea, et al., Appl. Cryst. 42 (2009) 339-341.

[4] G. M. Sheldrick, Acta Cryst. C 71 (2015) 3-8.

[5] Brandenburg, K. Diamond, 2010.

[6] Epifanovsky, A. T. B. Gilbert, X. Feng, J. Lee, Y. Mao, N. Mardirossian, P. Pokhilko, A. F. White, M. P. Coons, A. L. Dempwolff, Z. Gan, D. Hait, P. R. Horn, L. D. Jacobson, I. Kaliman, J. Kussmann, A. W. Lange, K. U. Lao, D. S. Levine, J. Liu, S. C. McKenzie, A. F. Morrison, K. D. Nanda, F. Plasser, D. R. Rehn, M. L. Vidal, Z.-Q. You, Y. Zhu, B. Alam, B. J. Albrecht, et al., J. Chem. Phys. 2021, 155, 084801.

[7] Wu, B. Kaduk, T. Van Voorhis. J. Chem. Phys. 2009, 130, 034109.

[8] Lu, F. Chen, Multiwfn: A multifunctional wavefunction analyzer. J. Comput. Chem. 2012, 33, 580.

[9] D. Rais, J. Yau, D. M. P. Mingos, R. Vilar, A. J. P. White and D. J. Williams, Angew. Chem., Int. Ed., 2001, 40, 3464-3467.

[10] D. Rais, D. M. P. Mingos, R. Vilar, A. J. P. White and D. J. Williams, J. Organomet. Chem., 2002, 652, 87-93.